

Constraining dark energy with cross-correlated CMB and Large Scale Structure data

Pier-Stefano Corasaniti,^{1,*} Tommaso Giannantonio,^{2,†} and Alessandro Melchiorri^{3,‡}

¹*ISCAP, Columbia University, 550 West 120th Street, New York, NY, 10027 (USA)*

²*Dipartimento di Fisica “G. Marconi”, Università di Roma “La Sapienza”, Ple Aldo Moro 5, 00185, Roma, Italy.*

³*Dipartimento di Fisica “G. Marconi”, Università di Roma “La Sapienza” and INFN, sezione di Roma, Ple Aldo Moro 5, 00185, Roma, Italy.*

We investigate the possibility of constraining dark energy with the Integrated Sachs Wolfe effect recently detected by cross-correlating the WMAP maps with several Large Scale Structure surveys. In agreement with previous works, we found that, under the assumption of a flat universe, the ISW signal is a promising tool for constraining dark energy. Current available data put weak limits on a constant dark energy equation of state w . We also find no constraints on the dark energy sound speed c_e^2 . For quintessence-like dark energy ($c_e^2 = 1$) we find $w < -0.53$, while tighter bounds are possible only if the dark energy is “clustered” ($c_e^2 = 0$), in such a case $-1.94 < w < -0.63$ at 2σ . Better measurements of the CMB-LSS correlation will be possible with the next generation of deep redshift surveys. This will provide independent constraints on the dark energy which are alternative to those usually inferred from CMB and SN-Ia data.

PACS numbers: 98.70.vc,98.80.Es

I. INTRODUCTION

The recent Wilkinson Microwave Anisotropy Probe (WMAP) satellite measurements of the Cosmic Microwave Background (CMB) anisotropy spectra provide an accurate determination of several cosmological parameters [1]. In combination with complementary results from galaxy surveys [2, 3], these data strongly suggest that the present energy budget of the universe is dominated by an exotic form of matter which is also responsible for the present phase of acceleration as directly inferred from measurements of luminosity distance to Supernova type Ia [4].

The presence of a cosmological constant term Λ in Einstein’s equation of General Relativity (GR) is the simplest explanation for dark energy. Remarkably the Λ cold dark matter scenario (Λ CDM) is the minimal model to consistently account for all observations and therefore has emerged as the standard model of cosmology.

The WMAP temperature anisotropy maps have been also cross-correlated with several surveys of Large Scale Structure (LSS) distribution and a positive correlation signal has been detected [5, 6, 7, 8, 9]. This is indeed another success of the Λ CDM model since the existence of a positive correlation was already predicted nearly a decade ago by Crittenden and Turok as a test of flat Λ -cosmologies [10].

Despite the simplicity of this concordance model, the nature of dark energy is far from being understood. In fact the existence of a small non-vanishing cosmological constant Λ arises questions to which present theoretical particle physics has found no consistent explanation. On

the other hand more exotic forms of matter such a scalar field cannot be *a priori* excluded. They have been proposed in several context as candidate for dark energy [11, 12, 13, 14, 15] and found to be consistent with current observations [16]. Alternatively in a number of scenarios it has been suggested that what appears as a dark energy component could be a manifestation of a modified theory of gravity or a consequence of spatial extra dimensions [17]. In this paper we will consider only GR gravity with a dark energy fluid whose energy momentum tensor violates the strong energy condition.

Within this framework the dark energy and the cosmological constant differs for two main aspects: the latter behaves as a homogeneous fluid with a constant energy density, while the former is a non-homogeneous fluid with a time dependent energy density and pressure. A simple way of describing these models is by specifying the equation of state $w = p_{DE}/\rho_{DE}$, where p_{DE} is the pressure and ρ_{DE} is the energy density. The cosmological constant corresponds to the specific constant value $w = -1$, while a general dark energy fluid may have a time dependent equation of state $w(t)$. General covariance requires Λ to be a homogeneous component, while dishomogeneities may occur in fluids with $w \neq -1$. The clustering properties of different dark energy models can be parameterized by an effective sound speed defined as the ratio between the pressure to density perturbations in the rest frame of dark energy, $c_e^2 = \delta p_{DE}/\delta \rho_{DE}$ [18]. Since we lack of a consistent theoretical formulation of dark energy we are left with constraining some phenomenological motivated form of $w(t)$ and c_e^2 .

The cross-correlation between CMB and LSS offers a new complementary way of constraining these parameters [19, 20, 21, 22, 23]. In fact the correlation between these data sets is consequence of the Integrated Sachs-Wolfe effect [24], which has been shown to be a sensitive probe of the evolution and clustering of dark energy [25, 26]. It is therefore timely to investigate whether cur-

*Electronic address: pierste@phys.columbia.edu

†Electronic address: tommaso.giannantonio@roma1.infn.it

‡Electronic address: alessandro.melchiorri@roma1.infn.it

rent measurements of the CMB-LSS correlation can already provide some novel constraints on the dark energy properties.

The paper is organized as follows : in Sec. II we introduce the ISW-correlation and study its dependence on dark energy. In Sec. III we describe the data analysis. In Sec. IV we discuss the results and finally we draw our conclusions in Sec. V.

II. THEORY

In a flat dark energy dominated universe the gravitational potentials associated with the large scale structures decay as consequence of the accelerated phase of expansion. CMB photons which cross these regions acquire a shift which generates temperature anisotropies. This is the so called Integrated Sachs-Wolfe (ISW) effect [24]. A natural consequence of this mechanism is that if there is a clump of matter, such as a cluster of galaxies in a given direction of the sky, we are likely to observe a spot in the corresponding direction of the CMB provided that the CMB photons have crossed that region during the accelerated epoch. We therefore expect to measure a positive angular correlation between CMB temperature anisotropy maps and surveys of the large scale structures.

The ISW temperature fluctuation, Δ_{ISW} , in the direction $\hat{\gamma}_1$ is given by:

$$\Delta_{ISW}(\hat{\gamma}_1) = -2 \int e^{-\tau(z)} \frac{d\Phi}{dz}(\hat{\gamma}_1, z) dz, \quad (1)$$

where Φ is the Newtonian gauge gravitational potential and $e^{-\tau(z)}$ is the visibility function to account for a possible suppression due to early reionization.

The density contrast corresponding to a clump of luminous matter observed by a given survey in the direction $\hat{\gamma}_2$ is:

$$\delta_{LSS}(\hat{\gamma}_2) = b \int \phi(z) \delta_m(\hat{\gamma}_2, z) dz, \quad (2)$$

with δ_m the matter density perturbation, b the galaxy bias and $\phi(z)$ is the selection function of the survey.

The 2-point angular cross-correlation is defined as

$$C^X(\theta) = \langle \Delta_{ISW}(\hat{\gamma}_1) \delta_{LSS}(\hat{\gamma}_2) \rangle, \quad (3)$$

where the angular brackets denote the average over the ensemble and $\theta = |\hat{\gamma}_1 - \hat{\gamma}_2|$. For computational purposes it is convenient to decompose $C^X(\theta)$ into the Legendre series such that,

$$C^X(\theta) = \sum_{l=2}^{\infty} \frac{2l+1}{4\pi} C_l^X P_l(\cos(\theta)), \quad (4)$$

where $P_l(\cos \theta)$ are the Legendre polynomials and C_l^X is the cross-correlation power spectrum given by [22, 23]:

$$C_l^X = 4\pi \frac{9}{25} \int \frac{dk}{k} \Delta_{\mathcal{R}}^2 I_l^{ISW}(k) I_l^{LSS}(k), \quad (5)$$

where $\Delta_{\mathcal{R}}^2$ is the primordial power spectrum. The integrand functions $I_l^{ISW}(k)$ and $I_l^{LSS}(k)$ are defined respectively as:

$$I_l^{ISW}(k) = -2 \int e^{-\tau(z)} \frac{d\Phi_k}{dz} j_l[kr(z)] dz \quad (6)$$

$$I_l^{LSS}(k) = b \int \phi(z) \delta_m^k(z) j_l[kr(z)] dz, \quad (7)$$

where Φ_k and δ_m^k are the Fourier components of the gravitational potential and matter perturbation respectively, $j_l[kr(z)]$ are the spherical Bessel functions and $r(z)$ is the comoving distance at redshift z .

Direct measurements of the cross-power spectrum C_l^X are more robust for likelihood parameter estimation since these data would be less correlated than measurements of $C^X(\theta)$. However current observations provide only estimates of the angular cross-correlation function, for this reason we focus on $C^X(\theta)$.

In order to better illustrate the model dependence of the ISW we compute the angular cross-correlation function for different values of w and c_e^2 . We first compute the cross-power spectrum of a given model using a properly modified version of CMBFAST code [27], then we evaluate $C^X(\theta)$ using Eq. (4). In this way the monopole and dipole contribution to the angular correlation function are subtracted by construction. We have implemented the dark energy perturbation equations as described in [28]. In what follows we assume a flat universe with Hubble parameter $h = 0.68$, $\Omega_{DE} = 0.7$, baryon density $\Omega_b h^2 = 0.024$, scalar spectral index $n_s = 1$, no reionization. The amplitude of the primordial fluctuations $A_s = 0.86$ (as defined in [29]) and the bias $b = 1$. We consider a Gaussian selection function peaked at $z = 0.1$ with variance $\sigma_\phi = 0.15$.

In Figure 1a we plot the angular cross-correlation for the case $c_e^2 = 1$ and in Figure 1b for $c_e^2 = 0$. The different lines correspond to $w = -0.8$ (solid), $w = -0.4$ (long dash-dot) and $w = -4$ (short dash).

We notice that at small angles the angular cross-correlation is characterized by a nearly constant plateau, while it rapidly vanishes at larger angles ($\theta > 10^\circ$). The overall amplitude of the signal up to angles $\theta \sim few^\circ$ is particularly sensitive to both w and c_e^2 . This can be better seen in Figure 1c and Figure 1d where we plot the amplitude of cross-correlation at the plateau, $C^X(0.3^\circ)$, as function of w in the case $c_e^2 = 1$ and $c_e^2 = 0$ respectively.

For $c_e^2 = 1$, the amplitude has a maximum around $w = -1$ and slowly decreases for decreasing values of w , while it rapidly falls to zero for $w \rightarrow 0$ (Fig. 1c). This is because the dark energy contribution to the ISW effect is mainly due to the background expansion. In fact for models with $w > -1$, as $w \rightarrow 0$ the dark energy driven expansion is less accelerated and tends to the matter dominated behavior. Hence the variation of the gravitational potentials is smaller and consequently produces a negligible amount of ISW as $w \rightarrow 0$. Similarly for models with $w < -1$, the dark energy affects the expansion later

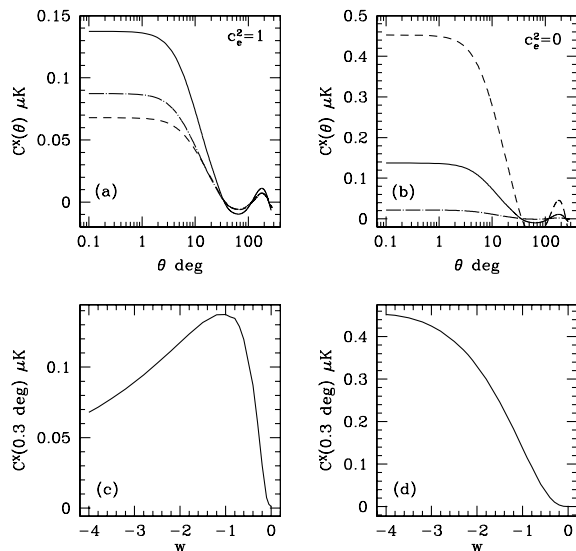


FIG. 1: Angular cross-correlation function for $c_e^2 = 1$ (a) and $c_e^2 = 0$ (b), the different lines corresponds to $w = -0.8$ (solid), $w = -0.4$ (long dash-dot) and $w = -4$ (short dash). Amplitude of the angular cross-correlation at the plateau as function of w for $c_e^2 = 1$ (c) and $c_e^2 = 0$ (d).

than in models with $w \geq -1$. This effectively extends the period of matter domination which leads to a lower ISW signal.

Since a smaller ISW signal can be compensated by increasing the amount of dark energy density Ω_{DE} , we expect a precise degeneracy line in the $\Omega_{DE} - w$ plane. In particular lower negative values of w will be counterbalanced by higher values of Ω_{DE} .

On the contrary for $c_e^2 = 0$, the amplitude of the cross-correlation is a monotonic decreasing function of w (Fig. 1d). In this case the decay of the gravitational potential is sensitive to the clustering of dark energy which is more effective as w decreases. Thus the amplitude of the ISW increases as w decreases [28, 30]. We therefore expect the degeneracy in the $\Omega_{DE} - w$ plane to be orthogonal to the previous case. In fact increasing Ω_{DE} will compensate for larger values of w .

This trend hold independently of the selection function as long as it is centered in a range of redshifts up $z \sim 0.7 - 0.8$ for models with $w \geq -1$. However one might expect this to not be the general situation in the case of dark energy models with a time dependent equation of state [23].

In Figure 2 we plot the amplitude of the angular cross-correlation at the plateau as function of the redshift. We have used a Gaussian function centered at different redshifts in steps of 0.1 and with a width $\sigma_\phi = 0.05$. The upper (lower) panel shows the case $c_e^2 = 1$ ($c_e^2 = 0$), the different lines correspond to the same models as in Figure 1. It can be seen that for $z \gtrsim 0.2$ the signal decreases

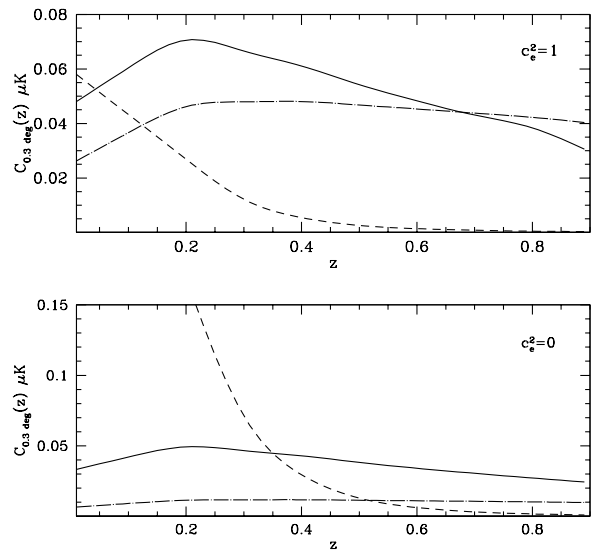


FIG. 2: Amplitude of the angular cross-correlation at the plateau as function of the redshift. A Gaussian selection function with width $\sigma_\phi = 0.05$ has been used. The different lines correspond to models as in Figure 1.

with the redshift in way that is strongly dependent on the dark energy parameters. Therefore redshift measurements of the cross-correlation are a potentially powerful tool to distinguish between different dark energy models.

We may also notice that having used a narrower selection function the amplitude of the signal is systematically smaller than that found in previous cases. For instance for $w = -0.8$ and $c_e^2 = 1$ we have $C(0.3^\circ) = 0.06\mu K$ at $z = 0.1$ (Fig.2 upper panel), which is smaller than $C(0.3^\circ) = 0.14\mu K$ (see Fig.1a) obtained using a wider selection function ($\sigma_\phi = 0.15$).

Hence a sharper selection function gives a smaller cross-correlation signal, eventually leading to larger uncertainties. On the other hand increasing the number of uncorrelated redshift bins would allow a better reconstruction of the redshift evolution of the cross-correlation.

This suggests that there could be an optimal way of designing a large scale structure survey which maximizes the discrimination power of the cross-correlation independently of the model of dark energy. This can be achieved using Integrated Parameter Space Optimization (IPSO) techniques [31]. We leave this interesting possibility to further investigation and we refer to [32] for a detailed analysis of dark energy parameter forecast from future cross-correlation data.

III. METHOD AND DATA

We perform a likelihood analysis using the collection of data presented in Gaztanaga *et al.* [33], which has

the advantage of being publicly available and easy to implement. These data consist of measurements of the average angular cross-correlation around $\theta = 5^\circ$ between WMAP temperature anisotropy maps and several LSS surveys. The angular average around $\theta = 5^\circ$ ensures that the signal is not contaminated by foregrounds such as the SZ or lensing effects which are relevant at smaller angles ($\theta \lesssim 1^\circ$). Taking the average does not wash out the sensitivity on the dark energy parameter since, as we have shown in Section II, the amplitude of the cross-correlation around $\theta = 5^\circ$ is still strongly dependent on the value of w and c_e^2 .

Possible systematic contaminants, such as extinction effects, seem not to affect these data and for a more detailed discussion we refer to [33].

The data span a range of redshift $0.1 < z \lesssim 1$ and for each redshift bin the data include an estimate of the galaxy bias with 20% errors. These biases are inferred by comparing the galaxy-galaxy correlation function of each experiment with the expectation of Λ CDM best fit model to WMAP power spectra.

The amplitude of the scalar density perturbation A_s is an overall normalization factor which we can marginalize over, on the contrary prior knowledge of the bias is required. In fact a scale and/or redshift dependent bias can in principle mimic the redshift evolution of the cross-correlation predicted by different dark energy models. It is therefore necessary to have an independent estimate of b , for instance by combining weak lensing information [34] or measurements of the matter power spectrum with the bispectrum [35].

One of the advantages of testing dark energy with the cross-correlation is that it is insensitive to other parameters which limits common dark energy parameter extraction analyses involving CMB temperature and polarization anisotropy spectra [36]. For instance the ISW correlation is not affected by a late reionization or by an extra background of relativistic particles which change the CMB spectra through the early-ISW (see e.g. [37]). The ISW-correlation is also independent of the amplitude of tensor modes and depends uniquely on the scalar perturbations, since a primordial background of gravity waves is uncorrelated with present large scale structure distribution.

There is little sensitivity to the scalar spectral index n_s , while the dependence on the baryon density Ω_b can be non-negligible. In fact the presence of baryons inhibits the growth of CDM fluctuations between matter-radiation equality and photon-baryon decoupling [38] causing the matter power spectrum to be suppressed on scales $k > k_{eq}$ for increasing values of Ω_b (k_{eq} is the scale which enters the horizon at the equality). Over the range of scales which contribute to the ISW-correlation ($k \sim 0.01$) the sensitivity on Ω_b is still present. In order to limit the number of likelihood parameters we therefore assume a Gaussian prior on the baryon density $\Omega_b h^2 = 0.0216 \pm 0.002$ consistent with WMAP and Big-Bang Nucleosynthesis bounds and consider the following

set parameters: the matter density Ω_m , the Hubble constant h , the equation of state w and the sound speed of dark energy c_e^2 . We assume a scale invariant primordial spectrum $n_s = 1$ and fix the optical depth to WMAP best fit value $\tau = 0.17$ (again the ISW is not particularly affected by a change in those parameters). We marginalize over the normalization amplitude A_s , although we found no difference assuming the WMAP value. In fact changing A_s shifts the overall amplitude of the angular cross-correlation of the same amount over different redshifts but it does not change the redshift dependence of the signal.

Since the experimental data are corrected for the bias by comparing the measured galaxy-galaxy correlation function in each redshift bin to the WMAP best fit model, we rescale these biases to each of the dark energy model in our database as described in [33].

We compute for each theoretical model the angular cross-correlation as described in Sec. II using the selection function

$$\phi^i(z) \sim z^2 \exp[-(z/\bar{z}_i)^{1.5}], \quad (8)$$

where \bar{z}_i is the median redshift of the i -th survey. Then following [33], we compute the average cross-correlation in the i -th bin, \bar{C}_i^X , around $\theta \sim 5^\circ$.

The data points are an average over angles and are inferred from surveys whose selection functions may overlap in redshift space, hence they are not independent measurements and indeed are affected by a certain degree of correlation. Since we have no access to the raw data we have no way of accounting for the first type of correlation, while using Eq. (8) we can estimate the correlation between different redshift bins. We compute the correlation matrix $\rho = \{\rho_{ij}\}$, where ρ_{ij} is the fraction of overlapping volume between the i -th and j -th surveys (i.e. the diagonal components are $\rho_{ii} = 1$). To be more conservative we have assumed that the different surveys cover the same fraction of sky, in general this is not the case and the fraction of overlapping volume can be smaller. We found that only two data points are highly correlated, since their selection functions overlap for about 70% in redshift space, while the correlation among the remaining data points are less than 20%.

We compute a likelihood function \mathcal{L} defined as

$$-2 \log \mathcal{L} = \chi^2 = \sum_{ij} (\bar{C}_i^X - \hat{C}_i^X) M_{ij}^{-1} (\bar{C}_j^X - \hat{C}_j^X), \quad (9)$$

where \hat{C}_i^X are the data and $M_{ij}^{-1} = \rho_{ij}/(\sigma_i \sigma_j)$ is our estimate of the inverse of the covariance matrix, with σ_i the measured uncertainty in the i -th bin.

We also use the SN-Ia ‘‘Gold’’ data [39] to derive complementary constraints on the dark energy parameters and compare with those derived from the ISW correlation.

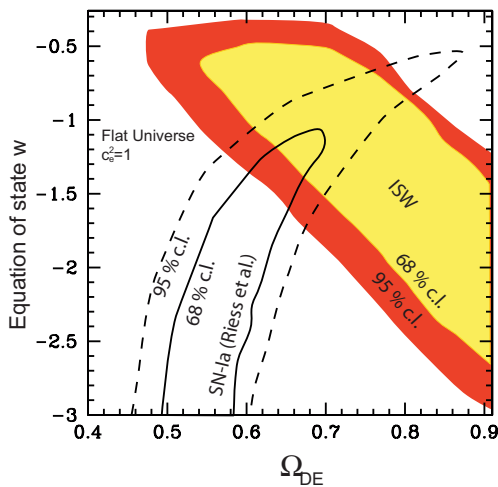


FIG. 3: Two-dimensional marginalized likelihoods on $\Omega_{DE} - w$. The yellow and red area correspond to 1 and 2σ limits inferred from the ISW data for $c_e^2 = 1$. Solid and dash lines represent the 1 and 2σ contours from the SN-Ia data.

IV. RESULTS

We now discuss the results of the likelihood analysis and show the marginalized constraints on the dark energy parameters. As expected we found that the results depend on the dark energy clustering. For instance in Figure 3 and 4 we plot the two-dimensional marginalized likelihoods in the $\Omega_{DE} - w$ plane for $c_e^2 = 1$ and $c_e^2 = 0$ respectively. The yellow and red contours correspond to 1 and 2σ limits. We also plot the marginalized likelihood inferred from the SN-Ia data.

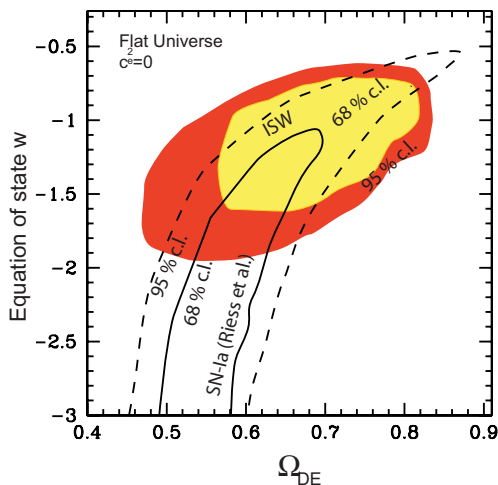


FIG. 4: As in Figure 3 with $c_e^2 = 0$ prior.

It appears evident that the derived limits on w strongly depend on the prior value of c_e^2 . In particular varying c_e^2 changes the direction of the degeneracy between Ω_{DE} and w . This is a natural consequence of the discussion presented in Section II. Namely, for $c_e^2 = 1$ decreasing

w causes a lower ISW signal which can be compensated by larger values of Ω_{DE} , while the opposite occurs for $c_e^2 = 0$. Therefore for $c_e^2 = 1$ the ISW data provide only a weak upper limit on the equation of state, $w < -0.53$ at 68% confidence level [43]. On the contrary assuming $c_e^2 = 0$ we obtain a tighter constraint $-1.94 < w < -0.63$ at 2σ .

We can also notice that for $c_e^2 = 0$ the combination of the ISW likelihood with the SN-Ia one has little effect in determining w , since the $\Omega_{DE} - w$ degeneracy of the luminosity distance lies in the same direction of the ISW cross-correlation. This is not the case for $c_e^2 = 1$, where the degeneracy lines are orthogonal. Therefore the combined likelihoods provide a more stringent bound, $-1.72 < w < -0.53$ at 95%.

These limits are stable assuming a standard prior on the matter density. For instance for $\Omega_m = 0.27 \pm 0.04$ we obtain $-1.51 < w < -0.72$ for $c_e^2 = 0$ and $-1.81 < w < -0.53$ for $c_e^2 = 1$ at 95%.

The constraints we have inferred so far would be 15 – 20% tighter if we had ignored the correlations amongst different redshift bins. In fact, as we have discussed in the previous Section, the level of correlation of current data is still non-negligible. On the contrary the next generation of surveys will be characterized by more localized selection functions and provide uncorrelated cross-correlation measurements.

In Figure 5 we plot the 5 data points and three different model predictions of the average angular cross-correlation normalized to the bias and the data. The solid line corresponds to the Λ CDM best fit model, we also plot a non-accelerating dark energy dominated model (long-dash line) and a phantom model (short-dash) which are disfavored by the data.

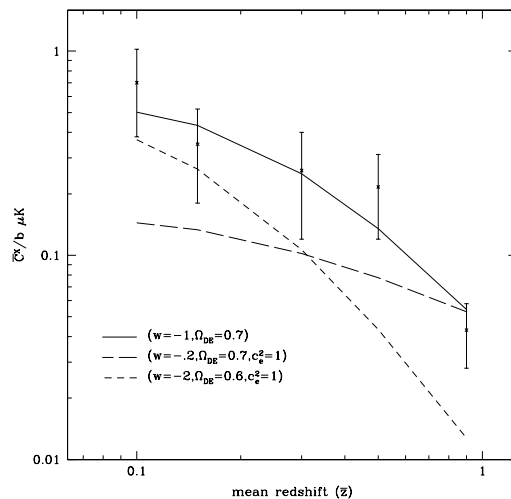


FIG. 5: Dots with errorbars are the different measurements of \bar{C}^X/b , the solid line corresponds to the Λ CDM best fit model, the long-dash and short-dash lines show the case ($w = -0.2, \Omega_{DE} = 0.7$) and ($w = -2, \Omega_{DE} = 0.6$) respectively.

In Figure 6 we plot the marginalized 1 and 2 σ contours in the $\log_{10} c_e^2 - w$ plane, as it can be seen the dark energy sound speed remains unconstrained. This is consistent with the results from the CMB data analysis by Weller and Lewis [30] and only at 2 σ with Bean and Dore [28].

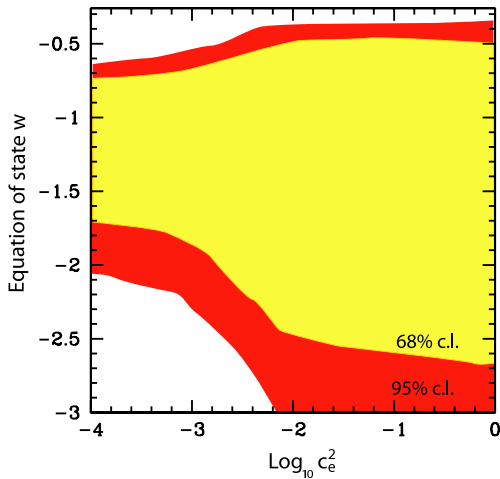


FIG. 6: Two-dimensional marginalized likelihood on $\log_{10} c_e^2 - w$ from ISW-correlation data. The yellow and red contours correspond to 1 and 2 σ limits.

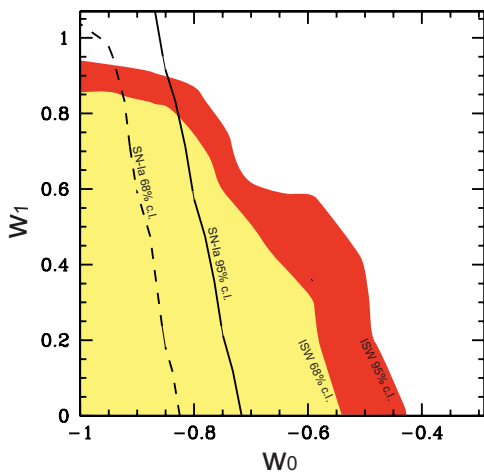


FIG. 7: 1 and 2 σ limits from ISW-correlation (yellow and red contours) and SN-Ia luminosity distance (dash and solid lines) on $w_0 - w_1$.

We have also extended our analysis to constrain a class of slowly varying dark energy models described by a parameterization of the equation of state which linear in the scale factor: $w(a) = w_0 + (1 - a)w_1$ [41].

This part should be considered as a simple exercise since current cross-correlation data are not accurate enough to allow us to constrain more than two parameters. We therefore assume an $\Omega_m = 0.3$ prior and we also restrict our analysis to models satisfying the Weak Energy Condition (WEC), $w_0 > -1$ and $0 < w_1 < 1$ such

that we can consistently account for the dark energy perturbations.

In Figure 7 we plot the marginalized 1 and 2 σ contours in $w_0 - w_1$ plane. We find that the cross-correlation data provide only weak upper limits on these parameters, $w_0 < -0.53$ and $w_1 < 0.84$. If we limit our analysis to models with $c_e^2 = 0$ the constraints are $w_0 < -0.82$ and $w_1 < 0.84$ at 68%. These limits are in agreement with similar constraints from SN-Ia as derived in previous analysis (see for instance [42]).

V. DISCUSSION

The cross-correlation between CMB and LSS data provides a new complementary way of testing dark energy. By isolating the ISW contribution to the CMB anisotropies, the correlation is a sensitive probe of the dark energy properties. In this paper we have studied its dependence on the dark energy equation of state w and sound speed c_e^2 . In particular we have shown that the redshift dependence of the cross-correlation signal may discriminate between different dark energy models and provide constraints on the dark energy parameters alternative to those inferred from cosmological distance measurements. In addition the ISW correlation is insensitive to a number of cosmological parameters which usually limits the dark energy parameter estimation from CMB data alone. A precise knowledge of the galaxy bias is necessary for this type of measurements to be competitive. In fact a redshift or scale dependent bias can in principle mimic the effect induced by dark energy.

We have also briefly reviewed the current observational status and inferred constraints on w and c_e^2 using the current limited datasets. We found that, even under several theoretical and optimistically experimental assumptions, the actual constraints are weak. However, the presence of a dark energy component is clearly significant in the data and interesting. The constraints on the equation of state strongly depends on the dark energy sound speed. In the case $c_e^2 = 1$ the ISW data provide only a weak upper limit on $w < -0.53$ at 1 σ , while tighter bounds are obtained assuming $c_e^2 = 0$. In agreement with previous independent works based on CMB data alone we found no constraints on the dark energy sound speed. Slowly varying dark energy models are also consistent with current ISW data but not significantly preferred. The upcoming deep redshift surveys such as LSST, KAOS or ALPACA are optimal datasets for studying the redshift evolution of the CMB-LSS correlation and provide alternative constraints on the dark energy parameters.

Acknowledgments

We are particularly grateful to Levon Pogonian for the very helpful suggestions and for checking our numerical results with his ISW-correlation code. We would like

to thank also Enrique Gaztanaga and Marilena Loverde for comments and discussions. P.S.C. is supported by

Columbia Academic Quality Fund, A.M. is supported by MURST through COFIN contract no. 2004027755.

-
- [1] D.N. Spergel *et al.*, *Astrophys. J. Supp.* **148**, 175 (2003).
 [2] W.J. Percival *et al.*, *Mon. Not. R. Astron. Soc.* **327**, 1297 (2001).
 [3] M. Tegmark *et al.*, *Astrophys. J.* **606**, 70 (2004).
 [4] S. Perlmutter *et al.*, *Astrophys. J.* **517**, 565 (1999); A.G. Riess *et al.*, *Astrophys. J.* **116**, 1009 (1998).
 [5] P. Fosalba, E. Gaztanaga and F.J. Castander, *Astrophys. J.* **89**, L597 (2003).
 [6] S.P. Boughn and R.G. Crittenden, *astro-ph/0305001*; S.P. Boughn and R.G. Crittenden, *Nature* **427**, 45 (2004).
 [7] R. Scranton *et al.*, *astro-ph/0307335*.
 [8] M.R. Nolta *et al.*, *Astrophys. J.* **608**, 10 (2004).
 [9] N. Afshordi, Y.S. Loh and M.A. Strauss, *Phys. Rev. D* **69**, 083524 (2004).
 [10] R.G. Crittenden and N. Turok, *Phys. Rev. Lett.* **76**, 575 (1996).
 [11] C. Wetterich, *Nucl. Phys.* **B302**, 668 (1988).
 [12] B. Ratra and P.J.E. Peebles, *Phys. Rev. D* **37**, 3406 (1988).
 [13] I. Zlatev, L. Wang and P.J. Steinhardt, *Phys. Rev. Lett.* **82**, 896 (1999).
 [14] C. Armendariz-Picon, V. Mukhanov and P.J. Steinhardt, *Phys. Rev. Lett.* **85**, 4438 (2000).
 [15] L. Amendola, *Phys. Rev. D* **62**, 043511 (2000).
 [16] P.S. Corasaniti and E.J. Copeland, *Phys. Rev. D* **65**, 043004 (2002); C. Baccigalupi, A. Balbi, S. Matarrese, F. Perrotta and N. Vittorio, *Phys. Rev. D* **65**, 063520 (2002); R. Bean and A. Melchiorri, *Phys. Rev. D* **65**, 041302(R) (2002); L. Amendola and C. Quercellini, *Phys. Rev. D* **68**, 023514 (2003).
 [17] S. Capozziello, S. Carloni and A. Troisi, *astro-ph/0303041*; S.M. Carroll, V. Duvvuri, M. Trodden and M.S. Turner, *Phys. Rev. D* **70**, 043528 (2004); G. Dvali, G. Gabadadze and M. Porrati, *Phys. Rev. Lett.* **B485**, 208 (2000); V. Sahni and Y.V. Shtanov, *JCAP* 0311, 014 (2003).
 [18] W. Hu, *Astrophys. J.* **506**, 485 (1998).
 [19] A. Cooray, *Phys. Rev. D* **65**, 103510 (2002).
 [20] N. Afshordi, *Phys. Rev. D* **70**, 083536 (2004).
 [21] W. Hu and R. Scranton, *Phys. Rev. D* **70**, 123002 (2004).
 [22] J. Garriga, L. Pogosian and T. Vachaspati, *Phys. Rev. D* **69**, 063511 (2004).
 [23] L. Pogosian, *astro-ph/0409059*.
 [24] R. Sachs and A. Wolfe, *Astrophys. J.* **147**, 73 (1967).
 [25] P.S. Corasaniti, B.A. Bassett, C. Ungarelli and E.J. Copeland, *Phys. Rev. Lett.* **90**, 091303 (2003).
 [26] A. Cooray, D. Huterer and D. Baumann, *Phys. Rev. D* **69**, 027301 (2004).
 [27] U. Seljak and M. Zaldarriaga, *Astrophys. J.* **469**, 437 (1996).
 [28] R. Bean and O. Dore, *Phys. Rev. D* **69**, 083503 (2004).
 [29] L. Verde *et al.*, *Astrophys. J. Supp.* **148**, 195 (2003);
 [30] J. Weller and A.M. Lewis, *Mon. Not. R. Astron. Soc.* **346**, 987 (2003).
 [31] B.A. Bassett, *astro-ph/0407201*; B.A. Bassett, D. Parkinson, R.C. Nichol, *astro-ph/0409266*.
 [32] L. Pogosian, P.S. Corasaniti, C. Stephan-Otto, R. Crittenden and R. Nichol, in preparation.
 [33] E. Gaztanaga, M. Manera, T. Multamaki, *astro-ph/0407022*.
 [34] W. Hu and B. Jain, *Phys. Rev. D* **70**, 043009 (2004).
 [35] D. Dolney, B. Jain and M. Takada, *astro-ph/0409445*.
 [36] P.S. Corasaniti, M. Kunz, D. Parkinson, E.J. Copeland and B.A. Bassett, *Phys. Rev. D* **70**, 083006 (2004).
 [37] R. Bowen, S. H. Hansen, A. Melchiorri, J. Silk and R. Trotta, *Mon. Not. Roy. Astron. Soc.* **334** (2002) 760.
 [38] W. Hu and N. Sugiyama, *Astrophys. J.* **471**, 542 (1996).
 [39] A.G. Riess *et al.*, *Astrophys. J.* **607**, 665 (2004).
 [40] P. Vielva, E. Martinez-Gonzalez and M. Tucci, *astro-ph/0408252*.
 [41] M. Chevallier and D. Polarski *Int. J. Mod. Phys. D* **10**, 213 (2001); E.V. Linder, *Phys. Rev. Lett.* **90**, 91301 (2003).
 [42] B.A. Bassett, P.S. Corasaniti and M. Kunz, *Astrophys. J.* **617**, L1 (2004).
 [43] The 1σ upper limit we found on w is much weaker than that obtained in [40], where the WMAP data have been correlated with the NVSS in the wavelet space.